[논 문] 한국재료학회지
Kor. J. Mater. Res.
Vol. 20, No. 5 (2010)

DOI: 10.3740/MRSK.2010.20.5.246

Photodegradation of MB on Fe/CNT-TiO_2 Composite Photocatalysts Under Visible Light

Kan Zhang, Ze-Da Meng, Jong Geun Choi and Won-Chun Oh†

Department of Advanced Materials & Science Engineering, Hanseo University, Chungnam 356-706, Korea

(Received April 22, 2010 : Received in revised form May 10, 2010 : Accepted May 11, 2010)

Abstract The composite photocatalysts of a Fe-modified carbon nanotube (CNT)-TiO_2 were synthesized by a two-step sol-gel method at high temperature. Its chemical composition and surface properties were investigated by BET surface area, scanning electron microscope (SEM), Transmission Electron Microscope (TEM), X-ray diffraction (XRD) and ultraviolet-visible (UV-Vis) spectroscopy. The results showed that the BET surface area was improved by modification of Fe, which was related to the adsorption capacity for each composite. Interesting thin layer aggregates of nanosized TiO_2 were observed from TEM images, probably stabilized by the presence of CNT, and the surface and structural characterization of the samples was carried out. The XRD results showed that the Fe/CNT-TiO_2 composites contained a mix of anatase and rutile forms of TiO_2 particles when the precursor is $TiOSO_4 \cdot xH_2O$ (TOS). An excellent photocatalytic activity of Fe/CNT-TiO_2 was obtained for the degradation of methylene blue (MB) under visible light irradiation. It was considered that Fe cation could be doped into the matrix of TiO_2, which could hinder the recombination rate of the excited electrons/holes. The photocatalytic activity of the composites was also found to depend on the presence of CNT. The synergistic effects among the Fe, CNT and TiO_2 components were responsible for improving the visible light photocatalytic activity.

Key words Fe/CNT-TiO_2 composites, modification, visible light, MB.

1. Introduction

Titanium dioxide as important photocatalyst has already been attracted most interests due to its specific optical and electronic properties, low cost, chemical stability and non-toxicity. However, first, because of the wide band gap of TiO_2, its practical application is limited for the need of an ultraviolet excitation source. Second, due to high recombination rate of the photogenerated electrons and holes, its photocatalytic activity is lower.[1-2] Hence, many attempts have been devoted to prepare TiO_2 photocatalyst that is capable of efficient utilization of visible light, Until now, several strategies including doping of TiO_2 with transition metals[3-4] anchoring organic dyes onto the surface of TiO_2[5-6] and doping with anionic nonmetals[7] have been reported. Among them, doping of TiO_2 with transition metal cations was investigated as a good tool to improve photocatalytic properties for enhancement of visible light response. Iron doped TiO_2 nanoparticles showed better photocatalytic activities than pure TiO_2 under visible light in many reports.[8-9] It was believed that Fe cations could act as shallow traps in the lattice of TiO_2, which was benefit to inhibit electron/hole recombination properties. Additionally, doping with nonmetallic species, such as N, C, and S also caused the photosensitization of TiO_2 in the visible light region.[10-12] Among various non-metals modified TiO_2, carbon-containing composites titania has been reported as a kind of promising photocatalyst. In a recent review, attention has been called to the fact that carbon nanotubes (CNT) are attractive and competitive catalyst supports when compared to carbon of many other kinds due to the combination of their electronic, adsorption, mechanical and thermal properties.[13] The unique electronic properties of CNT are that they can be either metallic or semiconducting, depending on their geometry.[14] Composites containing CNT are believed to provide many applications and exhibit cooperative or synergetic effects between the metal oxides and carbon phases.

More recently, the simultaneous doping of two kinds of atoms into TiO_2 has attracted considerable interest, since it could result in a higher photocatalytic activity and peculiar characteristics compared with single element doping into TiO_2. For example, Cong et al. reported that cooperation of nitrogen and iron cations led to the much narrowing of the band gap and greatly improved the photocatalytic activity in visible light region.[15] In our previous studies, co-doping TiO_2 with Pt or Y and CNT led to significant enhancement in photodegradation of methyl orange under visible light; the substitution of C for O was responsible for the band gap narrowing of TiO_2, and Pt and Y doping prevented the aggregation of powder in

†Corresponding author
E-Mail : wc_oh@hanseo.ac.kr (W. -C. Oh)

the process of preparation.[16-17] Tryba et al. prepared TiO_2 modified by carbon and iron photocatalyst by impregnating the powder TiO_2 with FeC_2O_4 solution and heating it at 400-800°C under flow of Ar gas.[18] They reported that the Fe-C-TiO_2 sample showed the higher photoactivity for phenol decomposition a under UV light and H_2O_2.[19-20] However, the ratio of Fe and C was fixed at definite value due to simultaneous introduction of Fe and C by one step reaction.

In the present paper, CNT and iron modified TiO_2 photocatalysts with enhanced photocatalytic activity for photodegradation of MB under visible light were obtained directly via two step sol-gel process at high temperature, respectively. The resulting TiO_2 photocatalysts were investigated using BET, SEM, TEM, XRD and UV-vis spectroscopy. The effect of single change of iron amounts on the properties of CNT modified TiO_2 was also investigated.

2. Experimental Procedure

2.1 Materials

As the support material, CNT were purchased from Carbon Nano-material Technology Co. (Korea), and used without further purification. *m*-chloroperbenzoic acid (MCPBA) was used as an oxidized reagent and purchased from Acros Organics (New Jersey, USA). Benzene (99.5%), which was used as an organic solvent, was purchased from Samchun Pure Chemical Co., Ltd. (Korea). Titanium (IV) oxysulfate hydrate ($TiOSO_4 \cdot xH_2O$ (TOS)) used as a titanium dioxide source for the preparation of the Fe/CNT-TiO_2 composite was purchased from Sigma-Aldrich Co., Ltd. (Germany), and $Fe(NO_3)_3 \cdot 9H_2O$ as the ferric source was purchased from Duksan Pure Chemical Co., Ltd. (Korea). The MB (analytical grade (≥ 99.99%)) was purchased from Duksan Pure Chemical Co., Ltd. (Korea).

2.2 Preparation

First step sol-gel process for preparation of Fe/CNT composite, 2 g MCPBA was dissolved in 80 mL benzene for preparing the oxidizing agent. Then, 20 mg CNT powder was put into the oxidizing agent solution, refluxed at 353 K for 6 h. The solid precipitates formed were dried at 363 K. The oxidized CNT was added to 10 mL different concentrations of Fe $(NO_3)_3 \cdot 9H_2O$ solution: 0.1, 0.25 and 0.5 M, and the mixtures were stirred for 24 h using a non-magnetic stirrer at room temperature, respectively. After the heat treatment at 773 K, we obtained the Fe/CNT. Second step sol-gel process for preparation of Fe/CNT-TiO_2 composite, the Fe/CNT was put into 1 M mixture of TOS and H_2O_2 (5%) solution. and then the mixed solution was stirred for 5 h in an air atmosphere. After stirring the solution transformed to gel state, and these gels were reacted at 923 K for 1 h. Then, the Fe/CNT-TiO_2 composite was obtained.

2.3 Characteristics

The BET surface area by N_2 adsorption method was measured at 77 K using a BET analyzer (Monosorb, USA). XRD (Shimadz XD-D1, Japan), the result was used to identify the crystallinity with Cu Kα radiation. SEM (JSM-5200 JOEL, Japan) was used to observe the surface state and structure of Fe/CNT-TiO_2 composites. TEM (JEOL, JEM-2010, Japan) at an acceleration voltage of 200 kV was used to investigate the size and distribution of the CNT deposited with ferric and titanium samples. UV-vis absorption parameters for the MB solution degraded by Fe/CNT-TiO_2 composites were recorded by a UV-vis (Optizen Pop Mecasys Co., Ltd., Korean) spectrophotometer. Used an 8W LED lamp ($\lambda > 420$ nm, Fawoo Technology, Korea) as visible light source was adopted to irradiate the MB solutions.

2.4 Photodegradation

The photocatalytic degradation was tested by Fe/CNT-TiO_2 composites powder and an aqueous solution of MB in a 100 mL glass container and then irradiation system with visible light (8W), which was used at the distance of 100 mm from the solution in dark box. The Fe/CNT-TiO_2 composites (0.05 g) were suspended in 50 mL of MB solution with a concentration of 1.0×10^{-5} M. Then, the mixed solution was placed in the dark for at least 2 h in order to establish an adsorption-desorption equilibrium, which was hereafter considered as the initial concentration (c_0) after dark adsorption. Then, experiments were carried out under visible light. Solution was then withdrawn regularly from the reactor by an order of 30 min, 60 min, 90 min, 120 min; afterwards, 10 mL of solution was taken out and immediately centrifuged to separate any suspended solid. The clean transparent solution was analyzed by using a UV-vis spectrophotometer. The blue color of the solution faded gradually with time due to the adsorption and decomposition of MB. And then the concentration of MB in the solution was determined as a function of irradiation time from the absorbance change at a wavelength of 660 nm.

3. Results and Discussion

3.1 BET surface area analysis.

The pure TiO_2, Fe/TiO_2, CNT-TiO_2 and Fe/CNT-TiO_2 composites were orderly denoted as T, FT, CT, FCT1, FCT2 and FCT3 and values of BET surface area of which are presented in Table 1 and. As the results of Table 1, The BET surface areas of pristine TiO_2 and Fe-TiO_2 were 8.3 and 11.9 m^2/g, respectively. While the BET surface areas of CNT-TiO_2 increased to 185.32 and Fe/CNT-TiO_2

Table 1. Nomenclatures and BET surface area of pure TiO_2, Fe/TiO_2, CNT-TiO_2 and Fe/CNT-TiO_2 composites.

Catalysts	Nomenclatures	S_{BET} (m^2/g)
Pure TiO_2	T	8.3
Fe/TiO_2	FT	11.9
CNT-TiO_2	CT	185.32
Fe/CNT-TiO_2 (0.1M)	FCT1	151.2
Fe/CNT-TiO_2 (0.25M)	FCT2	132.3
Fe/CNT-TiO_2 (0.5M)	FCT3	106.7

composites increased to average 130.1 m^2/g. When TiO_2 were modified by CNT and Fe-CNT compounds, it can be evidently seen that there was large change of the micropore size distribution for CNT-TiO_2 and Fe/CNT-TiO_2 composites compared to that of corresponding TiO_2. This indicated that the supported CNT were directly related to adsorption ability of TiO_2. In comparison of different Fe/CNT-TiO_2 composites, the specific surface area was gradually decreased with an increase of Fe contents in Fe/CNT-TiO_2 composites. It had been considered that the invaded Fe particles can be also blocked to microspores in CNT during first step sol-gel reaction process.

3.2 Morphology

Fig. 1 shows SEM images of the CNT-TiO_2 and Fe/CNT-TiO_2 composites. These may even look very similar in every detail. General morphology of CNT can be clearly observed in these micrographs. The TiO_2 grain structure was clearly visible with a great distribution on CNT surface due to considerable portion of TiO_2 attached in the 3-D matrix. Comparison of CNT-TiO_2 and Fe/CNT-TiO_2 composites, there was no significant difference. However, small amounts of TiO_2 particles were also aggregated to be bundles, which possibly are not well homogenized during vigorous stirring.

It was not clear to know exactly which Fe particles and CNT was presented within SEMs merely, so the TEM images were further collected to find out the morphology structure of Fe/CNT-TiO_2 composites in Fig. 2. The ordered microstructure of CNT-TiO_2 is kept unaffected partials of TiO_2 in Fig. 2(a). The black dots distributed in Fig. 2(b) corresponded to the Fe particles, there is evidence of the formation of doped TiO_2 outside the pores in some segments, this is possibly associated with the formed crystalline of Fe and TiO_2, which is finely agreed with the XRD results. A homogeneous dispersion of CNT in TiO_2 matrix implied a possible disappearance of CNT characteristic peaks in their XRD patterns.

3.3 Crystallite analysis

The wide angle XRD patterns of the Fe/CNT-TiO_2 com-

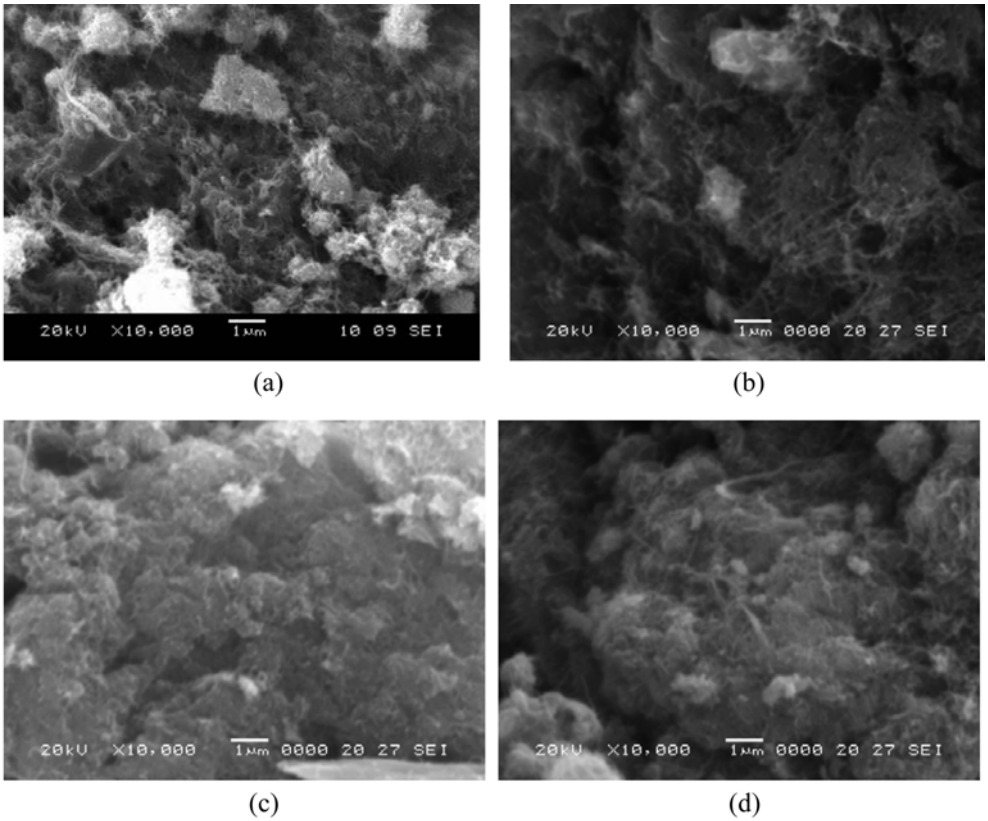

Fig. 1. SEM micrographs of CNT/TiO_2, Fe/CNT-TiO_2 composites: (a) CT, (b) FCT1, (c) FCT2 and (d) FCT3.

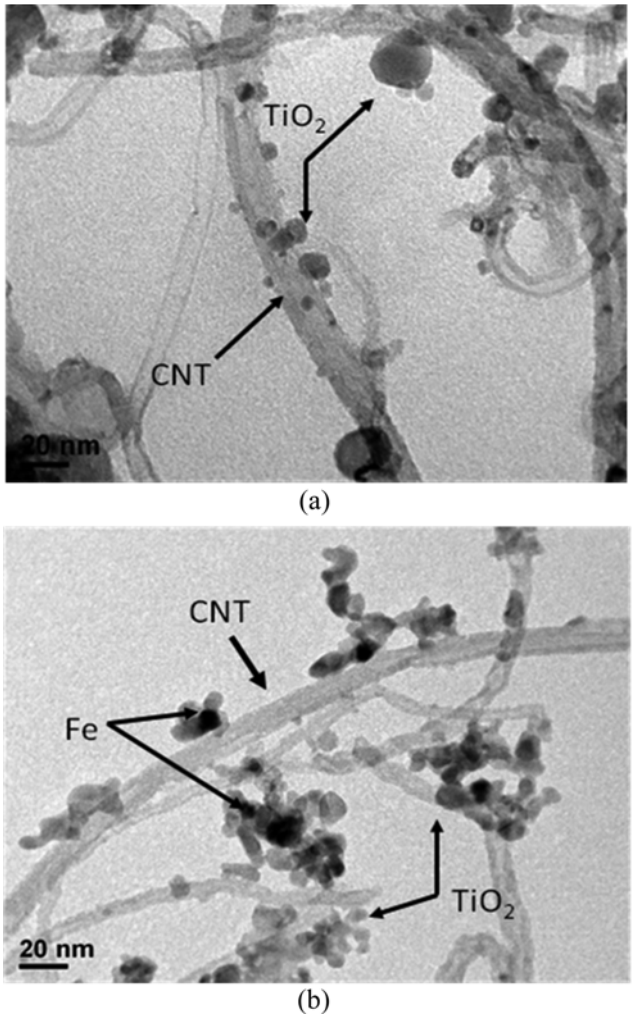

Fig. 2. TEM micrograph of the CNT/TiO_2 and Fe/CNT-TiO_2 composites: (a) CNT/TiO_2 and (b) Fe/CNT-TiO_2.

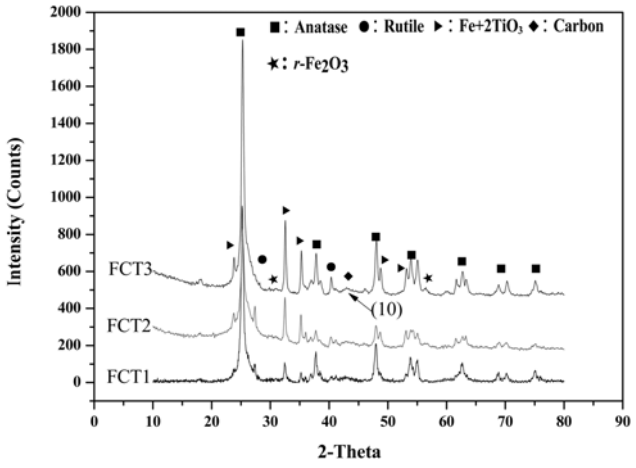

Fig. 3. XRD patterns of Fe/CNT-TiO_2 composite.

posites were investigated to analyze the effect of the Fe-CNT treatment on their crystallite phases. Fig. 3 shows the XRD pattern of the as-prepared Fe-CNT/TiO_2 composites. They showed that all the peaks of composites were distinguishable. The XRD results of Fe-CNT/TiO_2 composites illuminated that the CNT was coated with a mixed type of anatase and rutile TiO_2 particles. The major peaks were diffractions from (101), (004), (200) and (204) planes of anatase, and (110), (101), (111) and (211) of rutile. The results indicated that the phase transition from TOS to the anatase and rutile phases took place at 923K with formation of crystalline titania. The intense peaks of carbon correspond to the (002) reflection and to the (10) band. It could be noticed that the (101) anatase reflection overlaps the (002) reflection of carbon. Especially, pure maghemite (γ-Fe_2O_3) and uniform peaks of 'FeO + $2TiO_3$' could be obtained at Fe-CNT/TiO_2 composites, which indicated formation of the crystalline of Fe and TiO_2 due to reaction at high temperature.

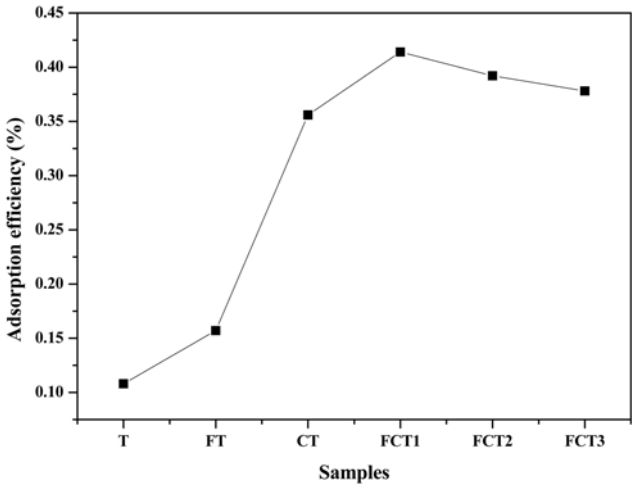

Fig. 4. Adsorption capability of pure TiO_2, Fe/TiO_2, CNT-TiO_2 and Fe/CNT-TiO_2 composites for MB dyes under dark condition.

3.4 Adsorption ability

To evaluate the adsorption ability of pure TiO_2, Fe/TiO_2, CNT-TiO_2 and Fe/CNT-TiO_2 composites, degradation of MB solution was run under dark condition which is graphically illustrated in Fig. 4. From the Fig. 4, it is clear that degradation of MB on CNT-TiO_2 and Fe/CNT-TiO_2 composites was higher than that of pure TiO_2 and Fe/TiO_2. This can be attributed to the large surface area of the CNT-TiO_2 and Fe/CNT-TiO_2 composites due to introduction of CNT, which correlates to a strong adsorption ability. However, the factors leading to the affected adsorption capacity should involve the change of the surface properties of the CNTs and surface particle dispersions. In addition, adsorption ability of the Fe/CNT-TiO_2 composites was slightly higher than that of the CNT-TiO_2 composite.

3.5 Photocatalytic activity

Fig. 5 shows the photocatalytic degradation curves of

MB over the pure TiO_2, Fe/TiO_2, $CNT\text{-}TiO_2$ and one kind of $Fe/CNT\text{-}TiO_2$ (FCT2) composites under visible light irradiation, And the photocatalytic degradation of MB with reaction time is first order as confirmed by the linear transforms of $-\ln(C_0/C)\sim t$, from which the apparent rate constants were obtained. The degradation rate of MB on pure TiO_2 under visible light irradiation was very low (3.18×10^{-4}), which can be attributed to the self-sensitization of MB.[21] Obviously, the photocatalytic activity of Fe/TiO_2 (2.83×10^{-3}) was superior to that of pure TiO_2 for the degradation of MB. The visible light reactivity of TiO_2 was significantly enhanced in presence of CNT (1.75×10^{-3}). As expected, over the above samples, the highest degradation ratio was occurred on Fe modified $CNT\text{-}TiO_2$ composite (4.99×10^{-3}).

In order to evaluate influence of different Fe contents for photocatalytic activity, the photocatalytic degradation curves of MB over the $Fe/CNT\text{-}TiO_2$ composites with different concentration of Fe under visible light irradiation are shown in Fig. 6. In comparison of three different $Fe/CNT\text{-}TiO_2$ composites, the degradation activity of FCT2 was higher than that of FCT1 and FCT3. It was considered that appropriate amount of the doped Fe in TiO_2 can effectively capture the photoinduced electrons and holes, which inhibited the combination of photoinduced carriers and improved the photocatalytic activity.

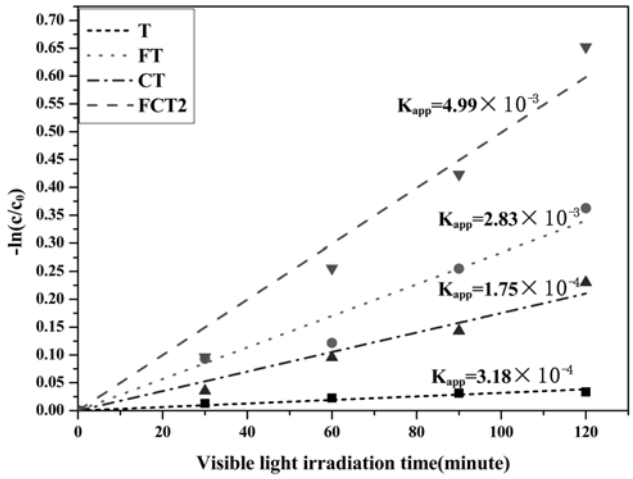

Fig. 5. $-\ln(C/C_0)$ versus time for pure TiO_2, Fe/TiO_2, $CNT\text{-}TiO_2$ and $Fe/CNT\text{-}TiO_2$ composites.

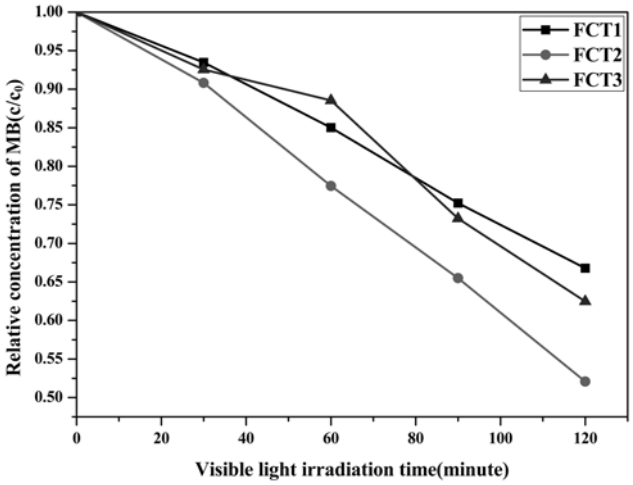

Fig. 6. Degradation of MB under visible light illumination for 120min in the presence of $Fe/CNT\text{-}TiO_2$ composites with different concentration of iron.

Interestingly, the rate constants of FCT2 were greater than the sum of the rate constants of respective Fe/TiO_2 and $CNT\text{-}TiO_2$ composites as shown in Fig. 5, which related to the cooperative effect between Fe-CNT and TiO_2. The synergistic effect may be attributed to three reasons: First, the specific surface area of $Fe/CNT\text{-}TiO_2$ composite was slightly larger than that of $CNT\text{-}TiO_2$ which may favor the adsorption of MB molecules as well as provide more possibly accessible active sites. Second, the peaks of "γ-Fe_2O_3" was significantly presented in their XRD pattern, which has a band gap of 2.2eV.[22] Therefore, When the $Fe/CNT\text{-}TiO_2$ composite was irradiated with visible light, the electrons in the valence band of γ-Fe_2O_3 particles were excited to the conduction band of TiO_2, leaving holes in the valence band of TiO_2. As a consequence, electrons in the valence bands of TiO_2 were injected into γ-Fe_2O_3 particles driven. Thus, we wish to postulate that an electron transfer in $Fe/CNT\text{-}TiO_2$ composite may takes place in the process of γ-$Fe_2O_3 \rightarrow TiO_2$ to form a narrower band gap. Third, both Fe and CNT species may improve the separation efficiency of photogenerated electrons and holes. In generally, Fe ions act as shallow electron-trapping centers (Eq. (1)), Subsequently, Fe^{2+} could be oxided to Fe^{3+} by transferring electrons to absorbed O_2 on the surface of TiO_2 (Eq. (2)) and a neighboring surface Ti^{4+} (Eq. (3)), which then lead to interfacial electron transfer (Eq. (4)).[23] While iron dopant content exceeds as shown FCT3, Fe ion becomes the recombination centers of the photoin-

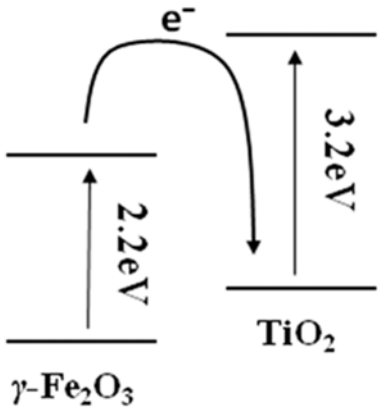

Scheme 1. Plausible electron transfer process.

duced electrons and holes, which is detrimental to photocatalytic reactions (Eqs. (5) and (6)).

$$Fe^{3+} + e^- \rightarrow Fe^{2+} \quad (1)$$
$$Fe^{2+} + O_2 \rightarrow Fe^{3+} \quad (2)$$
$$Fe^{3+} + Ti^{4+} \rightarrow Fe^{2+} + Ti^{3+} \quad (3)$$
$$Ti^{3+} + O_2 \rightarrow O_2^{-\bullet} \quad (4)$$
$$Fe^{3+} + e^- \rightarrow Fe^{2+} \quad (5)$$
$$Fe^{2+} + h^+ \rightarrow Fe^{3+} \quad (6)$$

Thus, as compared to FCT1, the photodegradation activity of FCT2 was significantly increased with an increase of Fe concentration. However, when the concentration of Fe ions becomes too large in FCT3, Fe ions can act as the recombination centers, resulting in the decrease of degradation activity.

4. Conclusion

The Fe modified CNT-TiO_2 composite photocatalysts were successfully synthesized by two step sol-gel process at high temperature. The Fe modified CNT-TiO_2 composite photocatalyst showed high specific surface areas, as well as more surface adsorbed ability, which contribute to their high photocatalytic activity for the degradation of MB under visible irradiation. It was found that Fe species are successfully incorporated into the crystal lattice of TiO_2, which can help the separation of photogenerated electron by trapping them temporarily and shallowly. In addition, the synergistic effects of CNT and Fe may efficiently promote the separation of photogenerated holes and electrons, and are responsible for high photodegradation of MB under visible light irradiation.

Reference

1. A. Fujishima, T. N. Rao and D. A. Tryk, J. Photochem. Photobiol. C., **1**, 1 (2000).
2. M. R. Hoffmann, S. T. Martin, W. Choi and D. W. Bahnemann, Chem. Rev., **95**, 69 (1995).
3. X. H. Wang, J. G. Li, H. Kamiyama, Y. Moriyoshi and T. Ishigaki, J. Phys. Chem. B., **110**, 6804 (2006).
4. S. Ghasemi, S. Rahimnejad, S. Rahman Setayesh, S. Rohani and M. R. Gholami, J. Hazard. Mater., **172**, 1573 (2009).
5. D. Liu, P. V. Kamat, K. G. Thomas, K. J. Thomas, S. Das and M. V. George, J. Chem. Phys., **106**, 6404 (1997).
6. K. Zhang and W. C. Oh, Kor. J. Mater. Res., **20**(1), 31 (2010).
7. R. Asahi, T. Morikawa, T. Ohwakl, K. Aoki and Y. Taga, Science., **293**, 269 (2001).
8. H. Kisch, L. Zang, C. Lange, W. F. Maier, C. Antonius and D. Meissner, Angew. Chem. Int. Ed., **37**, 3034 (1998).
9. K. Zhang, Z. D. Meng and W. C. Oh, Kor. J. Mater. Res., **20**(3), 117 (2010).
10. W. C. Oh and M. L. Chen, J. Cer. Proc. Res., **8**, 316 (2007).
11. T. Ohno, M. Akiyoshi, T. Umebayashi, K. Asai, T. MitSui and M. Matsumura, Appl. Catal. A: Gen., **265**, 115 (2004).
12. S. Y. Treschev, P. W. Chou, Y. H. Tseng, J. B. Wang, E. V. Perevedentseva and C. L. Cheng, Appl. Catal. B: Environ., **79**, 8 (2008).
13. E. Itoh, I. Suzuki and K. Miyairi, Jap. J. Appl. Phys., **44**, 636 (2005).
14. M. S. Dresselhaus, L. P. Biró, C. A. Bernardo, G. G. Tibbetts and P. Lambin, Carbon Filaments and Nanotubes: Common Origins, Differing Applications, Kulwer Academic Publishers, Dordrecht, 2000, p. 11.
15. Y. Cong, J. L. Zhang, F. Chen, M. Anpo and D. He, J. Phys. Chem. C., **111**, 10618 (2007).
16. F. J. Zhang, M. L. Chen, K. Zhang and W.C. Oh, Bull. Kor. Chem. Soc., **31**, 133 (2010).
17. W. C. Oh, F. J. Zhang, and M. L. Chen, J. Ind. Eng. Chem., **16**, 321 (2010).
18. B. Tryba, M. Toyoda, Chemosphere., **60**, 477 (2005).
19. B. Tryba, A. W. Morawski, M. Inagaki and M. Toyoda, Chemosphere., **64**, 1225 (2006).
20. B. Tryba, M. Piszcz, B. Grzmil, A. Pattek-Janczyk and A. W. Morawski, J. Hazard. Mater., **162**, 111 (2009).
21. C. Chen, W. Zhao, J. Li, J. Zhao and H. Hidaka, Environ. Sci. Technol., **36**, 3604 (2002).
22. X. W. Zhang and L. C. Lei, Appl. Sur. Sci., **254**, 2406 (2008).
23. K. Zhang, Z. D. Meng, W. B. Ko and W. C. Oh, Analy. Sci & Technol., **22**, 254 (2009).